Compactlike discrete breathers in systems with nonlinear and nonlocal dispersive terms

A. V. Gorbach and S. Flach
Max-Planck-Institut für Physik komplexer Systeme, Nöthnitzerstr. 38, Dresden 01187, Germany
(Received 28 February 2005; revised manuscript received 25 July 2005; published 8 November 2005)

Discrete breathers with purely anharmonic short-range interaction potentials localize *superexponentially* becoming compactlike. We analyze their spatial localization properties and their dynamical stability. Several branches of solutions are identified. One of them connects to the well-known Page and Sievers-Takeno lattice modes, another one connects with the compacton solutions of Rosenau. The absence of linear dispersion allows for extremely long-lived time-quasiperiodic localized excitations. Adding long-range anharmonic interactions leads to an extreme case of competition between length scales defining the spatial breather localization. We show that short- and long-range interaction terms competition results in the appearance of several characteristic crossover lengths and essentially breaks the concept of *compactness* of the corresponding discrete breathers.

DOI: 10.1103/PhysRevE.72.056607 PACS number(s): 05.45.Yv, 63.20.Pw, 63.20.Ry

I. INTRODUCTION

Energy localization due to a nonlinearity in dynamical systems has been observed for more than one century [1], and the effect of an exact balance between nonlinearity and linear dispersion of wave packets leading to the appearance of soliton excitations has become a paradigmatic example in nonlinear science which can be found in various textbooks. In the past decade remarkable achievements in the study of localized nonlinear excitations were made with the discovery of stable localized modes in spatially discrete translationally invariant Hamiltonian systems—*discrete breathers* (DBs) [2]. They have been proved to be generic *exact* time-periodic solutions of the corresponding coupled nonlinear ordinary differential equations, eventhough the latter are generally nonintegrable. It is worth mentioning that discrete breathers have been observed experimentally in various physical systems including coupled optical waveguide arrays [3–5], coupled Josephson junctions [6], micromechanical cantilever systems [7–9], antiferromagnetic crystals [10,11], high-T_c superconductors [12]. Discrete breathers are predicted also to exist in the dynamics of dusty plasma crystals [13].

Among the most important characteristics of a localized excitation are its localization length and the spatial decay characteristics of its amplitude. Although DBs can be localized practically on a single site, in most of the cases they have exponentially decaying tails (similar to their continuum counterparts—solitons). This is true if the interaction potentials are reasonably short ranged (see Ref. [14] for details). However, when an anharmonic interaction between adjacent sites is much stronger then the harmonic one, localized excitations can become even more compact. As it was demonstrated by Rosenau and Hyman [15,16], in continuous systems nonlinear localized excitations may compactify, i.e., gain strictly zero tails, under nonlinear dispersion. The same was conjectured for discrete systems [17], however, later it was shown that in discrete systems localized excitations cannot have an exact compact structure [18], but the tail decay follows a *superexponentional* law $e^{-a^{\exp bn}}$, provided that the interaction is purely short range. This fact was then confirmed numerically [19], and the corresponding breather solutions were coined *compactlike* [19] or *almost-compact* [20] DBs.

If compactlike breathers are dynamically stable, we may expect that localized perturbations of such solutions will lead to a quasiperiodic in time evolution, which will not induce a radiation of energy away from the breather. This is in contrast to the well-known existence of such a radiation for systems with linear dispersion [21]. There it appears due to the resonant overlap of combination frequencies of the internal perturbed breather dynamics with the spectrum of small amplitude plane waves. In the case of purely nonlinear dispersion the width of this spectrum is zero, and thus the origin of the radiation is removed. One expects then that perturbed compactlike breathers will not radiate energy away, giving rise to genuine *quasiperiodic* compactlike breathers.

Another important issue which might drastically change the rate of spatial decay in DB tails is the presence of long-range interactions, essential, e.g., in systems with weakly screened Coulomb interaction such as ionic crystals, or various biomolecules. Usually decaying slower than exponentially in space, long-range interactions introduce a crossover length as a result of competition of the two essentially different length scales [14]. They can also lead to the appearance of energy thresholds for DBs in some cases, where a pure short-range interaction would not be capable of producing any. In Ref. [22] it was demonstrated that the effect of length-scale competition with long-range algebraically and exponentially decaying interaction can lead to a different type of multistability of DBs, when in a certain model parameter regime several different types of DBs coexist having the same value of the spectral parameter (i.e., velocity or frequency).

It is the purpose of this paper to address the above-listed issues. The paper is organized as follows. In Sec. II we introduce the model. We demonstrate, that the specifically chosen nonlinear potentials allow one to completely separate temporal and spatial dependencies and thus significantly simplify the analysis of the problem. We derive the nonlinear coupled algebraic equations for the spatial profile of a solution and in addition an ordinary differential equation (Duffing equation) for the master function describing uniform oscillations of all the sites with time. In Sec. III we obtain the different types of discrete breather solutions. We demonstrate that in general the model supports two classes of discrete

breathers with completely different dynamical properties. We then study the linear stability properties of basic types of DBs and observe quasiperiodic localized excitations. In Sec. IV we reveal the effect of long-range interactions along the chain on properties of DB solutions. We show that the presence of nonlocal dispersive terms result in the appearance of several characteristic crossover lengths. We derive estimations for these crossover lengths, as well as asymptotes for amplitude distribution in DB tails, on the basis of a simple three-site model. In Sec. V we conclude.

II. MODEL

We consider a simple one-dimensional model of (nonlinearly) coupled oscillators with the following Hamiltonian:

$$H = \sum_n h_n \equiv \sum_n \left\{ \frac{\dot{u}_n^2}{2} + V(u_n) + \sum_{l>0} \frac{K}{4l^s}[(u_{n+l}-u_n)^4 + (u_{n-l}-u_n)^4] \right\}, \tag{1}$$

where $u_n(t)$ is the displacement of nth unit mass oscillator from its equilibrium position, the constant $s>0$ characterizes the rate of spatial decay of long-range interactions between oscillators, and $V(u_n)$ is given by

$$V(u_n) = \frac{u_n^2}{2} - \frac{u_n^4}{4}. \tag{2}$$

The equation of motion for the displacement of the nth oscillator from its equilibrium reads

$$\ddot{u}_n = K\sum_l \frac{1}{l^s}\{(u_{n+l}-u_n)^3 + (u_{n-l}-u_n)^3\} - u_n + u_n^3. \tag{3}$$

We note that while the interaction decays algebraically for any finite power s, in the limit $s\to\infty$ we recover the case of short-range nearest neighbor interaction.

The specifically chosen nonlinear potentials allow one to use the time-space separation technique [17,18], so that time-periodic solutions of Eq. (3) can be written in the form

$$u_n(t) = \phi_n G(t), \tag{4}$$

with time-independent amplitudes ϕ_n and a master function $G(t)$ describing *uniform oscillations* of all the sites. After substitution of the ansatz (4) into the Eqs. (3) the following equation for the function $G(t)$ is obtained:

$$\ddot{G} + G = -CG^3, \tag{5}$$

while the amplitudes ϕ_n satisfy algebraic equations:

$$C\phi_n = -K\sum_{l>0} \frac{1}{l^s}[(\phi_{n+l}-\phi_n)^3 + (\phi_{n-l}-\phi_n)^3] - \phi_n^3, \tag{6}$$

where C is an arbitrary separation constant. Its absolute value can be always chosen to be equal to unity [27].

While the dynamics of all the sites is governed by a unique function $G(t)$, which can be easily found by integrating Eq. (5), the spatial profile of possible solutions of Eqs. (3) is determined by Eqs. (6) being of main interest for us.

III. BASIC TYPES OF COMPACTLIKE DISCRETE BREATHERS

It is important to note that the dynamics of a DB, as well as its spatial profile, depend on the sign of C in Eqs. (5) and (6). This sign is fixed only for the case of uncoupled oscillators ($K=0$) and for small values of $K(C<0)$, while generally it can be arbitrary. As a consequence, for large enough values of K Eqs. (3) support *two classes* of DBs with different dynamical properties, since the sign of C defines the type of nonlinearity ("soft" or "hard") in Eq. (5) for the master function $G(t)$. DB solutions of different classes possess essentially different core structures. As a consequence, the impact of long-range interactions on DB tail structure is also different for these two classes of DBs.

A. Core structure of DBs

In order to understand how two different classes of solutions of Eqs. (3) appear, it is instructive to start with a simple case of three coupled oscillators. This simple model gives a rather good approximation for the sites of a DB core, which are practically not affected by the presence of long-range interactions. Here we restrict ourselves in considering only symmetric DBs centered at site $n=0$ (it is straightforward to modify this approximate model for more complicated types of *multisite* DBs). Therefore by putting $\phi_{-1}=\phi_1$ and $\phi_1=\kappa\phi_0$, we finally obtain from Eqs. (6) the following expression for the central site amplitude:

$$\phi_0^2 = -C\frac{1+2\kappa}{1+2\kappa^3(1-K)}, \tag{7}$$

while the coefficient κ is a root of the fourth-order polynomial equation

$$2K\kappa^4 - (4K+1)\kappa^3 + 3K\kappa^2 + (K+1)\kappa - K = 0. \tag{8}$$

For each given real value of κ obtained from Eq. (8) the sign of C is fixed and determined by the condition of non-negative valued right-hand side of Eq. (7).

In Fig. 1 the real roots of Eq. (8) are plotted in the range of the coupling constant $K\in[0,10]$. There exist two real nontrivial roots, whose absolute values stay below unity [and thus corresponding to single-site DBs with amplitudes of the central site ϕ_0 *greater* than those of the neighboring sites $\phi_{\pm1}$] in the whole interval of non-negative values of K up to $K\to+\infty$. One of these roots originates from $\kappa=0$ in the uncoupled limit (i.e., from a single-site excitation) and remains to be positive in the whole interval of K, see dashed line in Fig. 1. The corresponding family of DBs have a nonstaggered pattern of amplitudes ϕ_n—*in-phase* oscillations, see Fig. 2(a). The value of ϕ_0^2/C computed for this root from Eq. (7) is negative for $K\leqslant 2$ (see dashed line in the inset in Fig. 1), therefore one should choose $C=-1$ for this type of DBs in Eqs. (5) and (6). Thus DB solutions of Eq. (3) with a nonstaggered pattern should possess *soft* nonlinear properties, i.e., their amplitude decays with growing frequency, as it

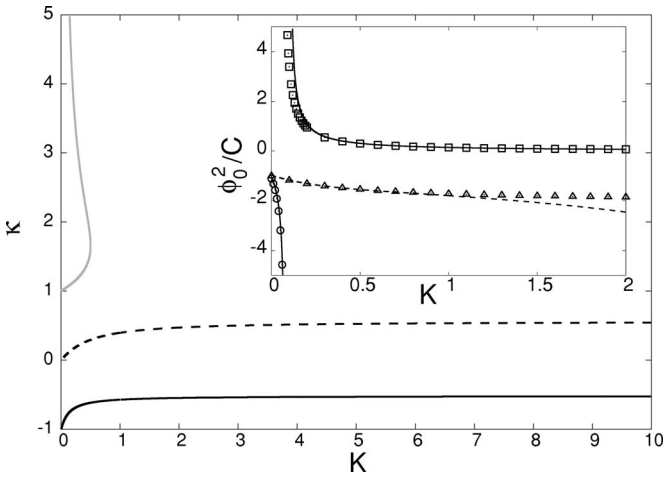

FIG. 1. Real roots of Eq. (8). The inset shows the corresponding values of ϕ_0^2/C computed from Eq. (7), squares, triangles and circles indicate the same quantity computed for the system of 201 coupled oscillators.

follows from the Eq. (5) with negative C. Here we mention that the quantity ϕ_0^2/C computed for the three-site model changes its sign above the value $K=2$. However, the comparison with numerically obtained solutions of Eq. (6) for a larger system size ($N=201$) indicates essential discrepancies when $K \gtrsim 1$ (see triangles in the inset in Fig. 1). It comes from the fact that a DB core of breathers with the nonstaggered profile extends while increasing K, approaching continuum compacton solutions [20] as $K \to +\infty$. Indeed, as shown in Fig. 2(a), while a DB core involves more and more sites with increasing K, its characteristic width in terms of the continuum coordinate $x=n/K^{0.25}$ remains to be fixed and demonstrates rather good agreement with the value $L_0 \approx 2.92$ reported for DBs in the continuum limit [20].

Another nontrivial real-valued root of Eq. (8) originates from $\kappa=-1$ in the uncoupled limit (i.e., from a staggered homogeneous excitation) and remains to be negative in the whole interval of K, see solid black line in Fig. 1. The corresponding DB family is characterized by a staggered profile in the core (while the tails have more complicated profile, as will be shown below), i.e., the central ($n=0$) and the neighboring ($n=\pm 1$) sites oscillate in *antiphase*. It is remarkable, that the corresponding value of ϕ_0^2/C changes its sign at $K=K_{cr} \approx 0.1$, see solid black lines in the inset in Fig. 1. Therefore for small enough values of the coupling constant $K<K_{cr}$ both staggered and nonstaggered types of DB solutions of Eq. (3) possess *soft* nonlinear properties, in accordance to the chosen type of the on-site nonlinear potential (2). The profile of the corresponding staggered-core DB solution at $K=0.07$ is shown in Fig. 2(b). Notably, all the tail sites perform inphase oscillations in this type of DBs, similar to the case of nonstaggered DBs described above. However, the central site oscillates in antiphase with all the rest of the lattice.

The competition between on- and intersite nonlinearities results in the change of dynamical behavior of the DBs with staggered core profile as the coupling becomes strong enough: The nonlinear term in Eq. (5) for the master function $G(t)$ becomes of the *hard* type for staggered DBs when $K>K_{cr}$. As the result, the amplitude of such a DB solution increases with growing frequency. The corresponding profile is shown in Fig. 2(c). In this type of staggered DBs all sites in the core perform antiphase oscillations. In the case of pure short-range interactions in the system, the staggered pattern persists for the whole spatial profile, including the breather tails. However, long-range interactions destroy the uniform staggered pattern, introducing a complicated domainlike structure in the breather tails, as will be explained below.

Unlike DBs with nonstaggered profile, the staggered core DBs stay localized on a few sites as K increases, therefore the three-site model gives a rather good approximation for larger size systems for arbitrarily large values of K (see squares in the inset in Fig. 1). Simultaneously, the amplitude of these DBs decreases as $K \to +\infty$ (for a fixed value of the frequency). However, we note that there is no limit in frequency (and therefore in energy) for this type of DB, since the master function $G(t)$ satisfies the Duffing equation (5) with the *hard* nonlinear term ($C=1$). Note also that as $K \to +\infty$, the influence of the intersite nonlinear interactions becomes more important than the effect of on-site nonlinearities for the oscillating in antiphase sites of the DB core. Therefore at large values of K the staggered-core DB asymptotically approaches the high-energy limit of discrete breather solutions in models with purely intersite nonlinearities (Fermi-Pasta-Ulam lattices) [23].

Thus for $K>K_{cr}$ Eqs. (3) support *two different classes* of DB solutions with *soft* and *hard* nonlinear properties, in what follows we will refer to such breather solutions as *S-type* and *H-type* DBs, respectively. The above discussed single-site DBs represent only particular (basic) members of these two classes of solutions. In general, one can constract more complicated localized *S*- and *H*-type solutions—*multisite* DBs. As an example, we mention here *two-site* DBs with two sites in the core oscillating with the same (maximum) amplitude, see gray lines and symbols in Fig. 2. The center of energy density distribution is located in-between two sites in these DBs, so that they can be viewed as translated half site single-site DBs.

Finally, we would like to remark, that the existence of the two different classes of DB solutions of Eqs. (3) is the result of a competition between soft nonlinearity of the on-site potential and hard nonlinear intersite interactions. Upon change the type of nonlinearity in the on-site potential [by changing the sign of the quartic term in Eq. (2)], only the *H*-type DBs with staggered core profile survive.

B. Linear stability

Different dynamical properties of DBs with staggered and nonstaggered core profiles result, in particular, in different stability properties of these excitations. In this section we perform linear stability analysis of basic types of *H*- and *S*-type DBs by studying the dynamical behavior of a small perturbation $\epsilon_n(t)$ to a given DB solution $\hat{u}_n(t)$. In order to construct a certain type of DB solution of Eq. (3), we solve numerically Eqs. (6) for the DB profile $\hat{\phi}_n(t)$ with a certain sign of the separation constant C (chosen in accordance to

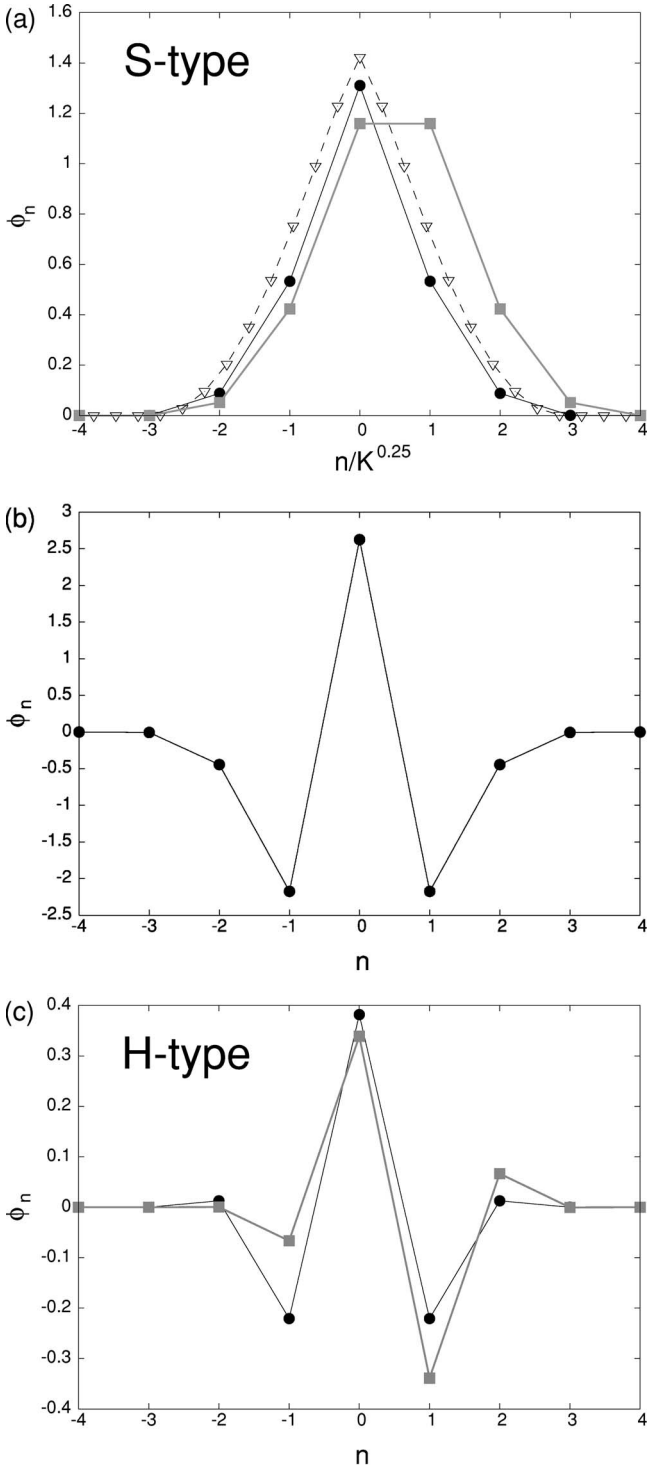

FIG. 2. Profiles of various types of single-site (black color) and two-site (gray color) DB solutions of Eq. (6): (a) nonstaggered DBs corresponding to the branch marked with triangles in the inset in Fig. 1 (*S*-type DBs), parameter values are $C=-1$, $K=1$ (circles, squares), and $K=100$ (triangles); (b) a staggered-core DB corresponding to the branch marked with circles in the inset in Fig. 1, parameter values are: $C=-1$, $K=0.07$ ($K<K_{cr}$); (c) staggered-core DBs corresponding to the branch marked with squares in the inset in Fig. 1 (*H*-type DBs), parameter values are $C=1$, $K=1$ ($K>K_{cr}$). The long-range decay rate is $s=100$, lines are provided to guide the eye.

the above performed analysis of DBs structure) and multiply it by a periodic solution $\hat{G}(t)$ of the Duffing equation (5), according to the ansatz (4). Because of the time-space separation (4), the stability properties remain qualitatively the same for the whole family of a given DB type with different frequencies $\Omega_B=2\pi/T_B$ [i.e., with different time-periodic functions $G(t+T_B)=G(t)$]. However, they might drastically change by varying the relative strength of the on-site and intersite nonlinearities controlled by the coupling constant K.

Thus once a given DB solution $\hat{u}_n(t)$ is obtained numerically, we add a small perturbation to it $u_n(t)=\hat{u}_n(t)+\epsilon_n(t)$ and linearize equations of motion Eqs. (3) with respect to $\epsilon_n(t)$:

$$\ddot{\epsilon}_n = 3K\sum_l \frac{1}{l^s}\{(\hat{u}_{n+l}-\hat{u}_n)^2(\epsilon_{n+l}-\epsilon_n)+(\hat{u}_{n-l}-\hat{u}_n)^2(\epsilon_{n-l}-\epsilon_n)\} - \epsilon_n + 3\hat{u}_n^2\epsilon_n. \tag{9}$$

In order to simplify the stability analysis, here we restrict ourselves in considering pure short-range interaction terms, thus we keep only the term with $l=1$ in the right-hand side of Eqs. (9), which corresponds to the limit $s\to\infty$. Being essential for DB tail characteristics, long-range interactions practically do not affect the core structure of a DB, provided that their decay rate s is sufficiently large ($s>3$). Therefore the impact of long-range interactions on stability properties of DBs is expected to be negligible.

The discrete breather acts as a parametic driver for small perturbations $\epsilon_n(t)$ with the period $T=T_B/2$ being the half period of the DB solution [i.e., the half period of a given solution $G(t)$ in Eq. (5)].

Equations (9) define a map

$$\begin{pmatrix}\vec{\dot{\epsilon}}(T)\\ \vec{\epsilon}(T)\end{pmatrix} = \mathcal{F}\begin{pmatrix}\vec{\dot{\epsilon}}(0)\\ \vec{\epsilon}(0)\end{pmatrix} \tag{10}$$

which maps the phase space of perturbations onto itself by integrating each point over the period T. Here we used the abbreviation $\vec{x}\equiv(x_1,x_2,\ldots,x_l,\ldots)$. The map (10) is characterized by a symplectic Floquet matrix $\mathcal{F}$, whose complex eigenvalues λ and eigenvectors $\vec{y}$ provide information about the stability of the DB [2]. Here we note that if all eigenvalues λ are by modulus 1, then the DB is linearly (marginally) *stable*. Otherwise perturbations exist which will grow in time (typically exponentially) and correspond to a linearly *unstable* DB. Upon changing a control parameter (e.g., the coupling constant K) stable DBs can become unstable (and vice versa). Such a change of stability is appearing because two (or more) Floquet eigenvalues collide on the unit circle and depart from it [2].

In Fig. 3(a) the typical Floquet spectrum is shown for a *S-type* single-site DB. All the eigenvalues λ can be divided into three subcategories: One pair of eigenvalues is always situated at $\exp(i\pi)$ [denoted by squares in the inset in Fig. 3(a)]; it corresponds to perturbations along the DB periodic orbit (phase mode) and along the corresponding family of DB solutions [2]. The period of these perturbations coincides with the DB period. In addition, there are quasidegenerated [28] bands of eigenvalues at $\lambda=\exp(\pm iT_B/2)$ [filled circles in

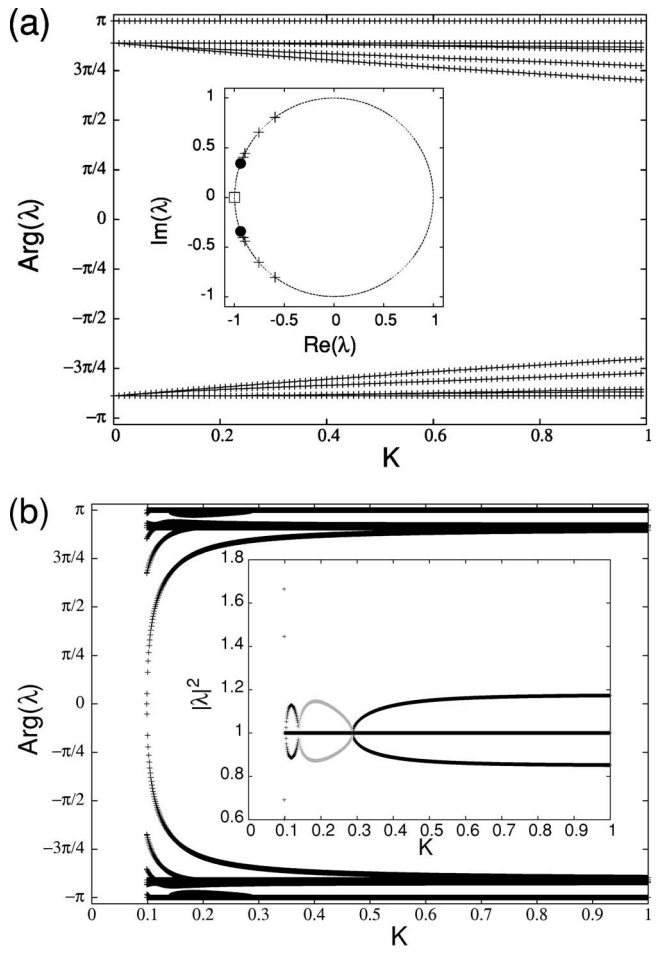

FIG. 3. Evolution of the arguments of Floquet eigenvalues λ with change of the coupling constant K for different types of single-site DBs: (a) S-type DB with the frequency $\Omega_B=0.9$. Inset shows the Floquet spectrum at $K=1$, the unit circle in the complex plane is indicated to guide the eye; (b) H-type DB with the frequency $\Omega_B=1.1$. Inset shows evolution of absolute values $|\lambda|^2$ with change of K. A pair of eigenvalues corresponding to the unstable depinning mode (see the main body text for the details) of the two-site DB is indicated with gray color.

the inset in Fig. 3(a)], which correspond to perturbations in breather tails. Such perturbations have characteristic frequency $\omega_l=1$ defined by the choice of the linear constant in the on-site potential (2), they would correspond to linear phonons if linear coupling between sites were introduced. Finally, there is a finite number of eigenvalue pairs bifurcating from the quasidegenerated bands, which correspond to perturbations of the DB core sites [crosses in the inset in Fig. 3(a)]. The number of such isolated pairs is proportional to the characteristic DB core size, it grows as the coupling constant K increases, see Fig. 3(a). While increasing the coupling constant K, these isolated pairs move on the unit circle and new pairs bifurcate from the quasidegenerated band, but they do not collide with each other and the nonstaggered type of DB remains linearly stable up to the continuum limit $K\rightarrow+\infty$.

Notably, the Floquet spectrum of the S-type two-site DB is qualitatively the same as the one of the single-site DB for any K. The only principal difference is that it has two degenerated pairs of eigenvalues at $\lambda=\exp(i\pi)$, since in the uncoupled limit $K=0$ the corresponding solution has two sites excited with equal amplitude. Usually such degeneracy of eigenvalues is lifted for any nonzero K, and one pair of eigenvalues is "pushed out" from $\lambda=\exp(i\pi)$ either along the real axis or along the unit circle. However, in the case of purely nonlinear interactions between sites the *symmetric* two-site DB "cuts" the effective linear chain (9) into two noninteracting halves. Therefore the additional degeneracy of eigenvalues corresponding to symmetric and antisymmetric perturbations with respect to the DB center remains for any K.

In contrast to the S-type DBs, the H-type single-site and two-site DBs are linearly stable only within certain windows of the coupling constant K values, see Fig. 3(b). Close to the critical value of the coupling constant $K=K_{cr}$, below which the H-type DBs do not exist, both single- and two-site H-type DBs experience strong instabilities connected with tangent bifurcations of these solutions with other ones, having more complicated spatial structure. In addition, there is another instability of a finite strength, appearing in certain windows of the parameter K, see inset in Fig. 3(b). In general, apart from several small intervals in K, for any given value of K only one of these two DB configurations is stable. The corresponding unstable perturbation—the "depinning" mode—"tilts" the single-site (two-site) DB towards the half site shifted stable two-site (single-site) one. Changing the coupling constant, the stable configuration varies from the two-site to single-site DB and back [at $K\approx0.15$ and $K\approx0.3$, see Fig. 3(b)], so that the *exchange of stability* process [25] is observed. This exchange of stability process can be connected to an exchange of the dominant roles between intersite and on-site nonlinearities. Indeed, typically for models with purely intersite nonlinearities (Fermi-Pasta-Ulam lattices) the basic stable configuration is the two-site DB [2,23]. In contrast, for models with weak coupling between sites and a nonlinear onsite potential in the form (2) (Klein-Gordon lattices) the single-site DB configuration is stable [2].

Of principal interest is an influence of the unstable depinning mode on the dynamical behavior of staggered-core DBs. A small perturbation along this mode is generally known to result in depinning of the unstable DB from its initial position. Depending on the relative Hamiltonian energy (1) of the perturbation ($\Delta H/H_{DB}$) and on the strength of instability of the depinning mode, the resulting behavior might vary from quasiperiodiclike oscillations between two neighboring unstable positions (in a well of the corresponding "Peierls-Nabarro potential") to quasiregular or even chaoticlike motion along the chain (see, e.g., Refs. [25,26]). Generally, the depinned DB resonates with linear phonons through its excited internal modes and starts to radiate energy. Therefore eventually it will be trapped again at some stable position or even disappear completely transferring totally its energy to excited delocalized phonons.

However, in the case of purely nonlinear dispersion there are no linear phonons in the system, and all possible linear resonances are suppressed. As a result, one can observe almost perfect quasiperiodic oscillations of perturbed unstable

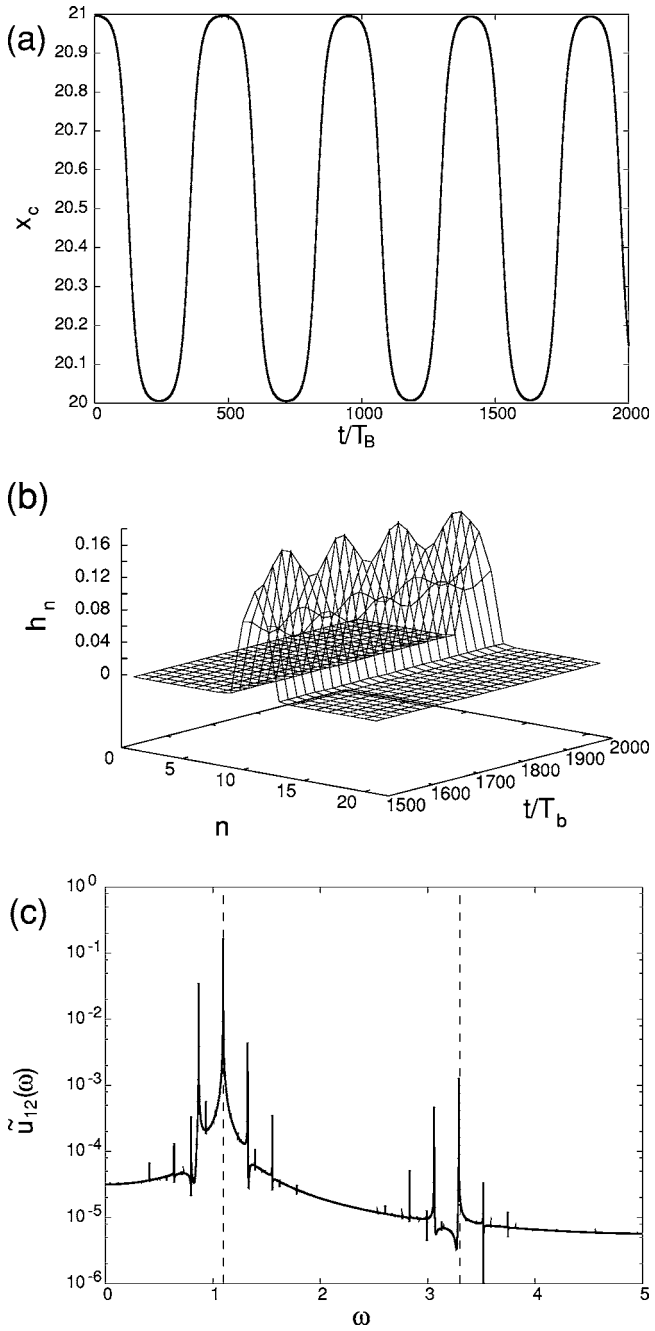

FIG. 4. Dynamics of a perturbed DB: (a) Position of the DB center x_c, calculated through the energy dencity h_n (1): $x_c=\Sigma_n(n\cdot h_n)/\Sigma_n h_n$. At time $t=0$ the single-site H-type DB ($\Omega_B=1.1, K=0.3$) was perturbed along the unstable depinning mode with the relative energy of perturbation $\Delta H/H_{DB}\sim 10^{-4}$; (b) energy density h_n (1) evolution in dynamics of the stable single-site H-type DB ($\Omega_B=1.1$, $K=0.2$) with a symmetric perturbation along one of the DB internal modes. The relative energy of perturbation $\Delta H/H_{DB}\sim 10^{-2}$; (c) the Fourier transform of $u_{12}(t)$ (the DB is centered at $n=11$) for the same dynamical simulation as in (b). Vertical dashed lines indicates the first and the third DB harmonics $\Omega_B=1.1$ and $3\Omega_B=3.3$.

DBs between two neighboring stable positions, see Fig. 4(a). Similar quasiperiodic behavior is observed in dynamics of a stable DB with perturbation along one of its internal modes,

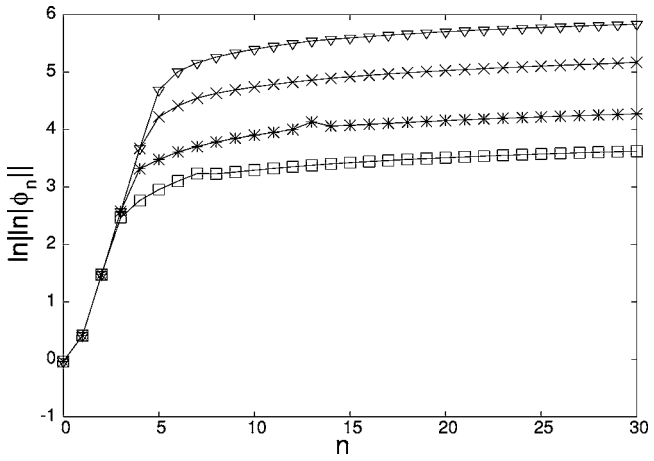

FIG. 5. Single-site H-type DB solutions of Eq. (6) with $C=1$ and $K=1$ for various exponents of the long-range interaction: $s=10$ (squares), $s=20$ (stars), $s=50$ (crosses), and $s=100$ (triangles).

see Figs. 4(b) and 4(c). In the latter case no detectable radiation (within the used double precision) of energy from the DB core was observed during dynamical simulation over 10^5 breather periods. In this respect, a one-dimensional Hamiltonian lattice with purely anharmonic interactions between sites (1) might be an interesting "toy model" to study more complicated *exact* DB solutions like quasiperiodic and moving discrete breathers.

IV. LONG-RANGE INTERACTIONS EFFECT

Let us now fix the value of $K=1$ and study the influence of long-range interactions on the spatial profile of a DB. In Fig. 5 the profiles of the H-type single-site DBs are shown for various values of the decay constant s. They were obtained by solving Eqs. (6) numerically with use of the standard Newton scheme [24] for the chain of $N=201$ oscillators ($-100<n<100$) with periodic boundary conditions [29]. Similarly to the case of nonlinear short-range interaction, the computed DBs have a compactlike structure with mainly three central sites oscillating (see Fig. 2). The other oscillators are almost at rest and can be considered as breather tails. The presence of long-range interactions breaks the uniform superexponential law of the spatial tail decay known for the case of pure short-range nonlinear interactions [18,19], introducing several crossover lengths.

For a few central sites, lying within the breather core, the forces due to the long-range interactions are negligible as compared to those due to the nearest-neighbor interactions. Thus the central part of a breather is practically not affected by the presence of long-range interactions. However, at some distance L_1 from the DB center interactions with the nearest neighbors (having small enough amplitudes) become of the same order as the long-range interactions with the DB core (central three sites having the highest amplitudes). This distance is the first crossover length, where the long-range interactions come into play. It can be roughly estimated by an assumption, that at the distance L_1 interactions with the

breather core sites are exactly compensated by interactions with the nearest neighbors. Thus keeping only the leading order terms in the sum in the right-hand side of Eq. (6) one obtains

$$-\frac{\phi_1^3}{(L_1-1)^s}=\phi_{L_1-1}^3. \tag{11}$$

Since for $|n|<L_1$ the relations between the amplitudes ϕ_n are practically the same as in the case of pure nearest-neighbor interactions, i.e., they follow the superexponential law $\phi_n\sim(-1)^n|\phi_1|^{\exp(\ln(3)|n-1|)}$, $1\leqslant|n|\leqslant L_1$, one can obtain from Eq. (11)

$$|\phi_1|^{\exp[3\ \ln\ 3(L_1-2)]-3}(L_1-1)^s=1. \tag{12}$$

In the limit of extremely large values of s the distance L_1 will be also large, and satisfy

$$L_1\sim\frac{\ln s}{\ln 3}+2. \tag{13}$$

Thus the first crossover length L_1 grows approximately logarithmically with s. The numerical results in Fig. 5 yield $L_1(s=10)\approx 3$, $L_1(s=20)\approx 4$, $L_1(s=50)\approx 5$, and $L_1(s=100)\approx 6$. They compare very well with the corresponding solutions of Eq. (12): 2.71, 3.46, 4.44, 5.17. Therefore even extremely fast (but still algebraically) decaying in space long-range interactions essentially destroy the concept of compactlike breathers, since only amplitudes of a few sites in the tails obey the superexponential law of decay, while the rest of the tail amplitudes decay much slower in space (following a power law, as will be shown below).

At large distances from the breather center $n\gg 1$ (due to the single-site DB symmetry around $n=0$ we consider here only non-negative values of n) the impact of short- and long-range interactions is exchanged: now the most powerful contribution comes from the interaction with the breather core, while nearest neighbors, due to their small amplitudes, practically do not affect the dynamics of a tail site. Thus for large n one can derive from Eq. (6) the following asymptote:

$$\phi_n\approx-\frac{K}{C}\left[\frac{\phi_0^3}{n^s}+\frac{\phi_1^3}{(n-1)^s}+\frac{\phi_1^3}{(n+1)^s}\right], \tag{14}$$

which in fact gives a rather good approximation for all tail sites starting from the first crossover point $n=L_1$ (see solid lines in Fig. 6). Note that only amplitudes of the two DB core sites and the sign of separation constant C are needed to obtain this asymptote for tail amplitude distribution. In this respect we found the simple three-site model, discussed in Sec. III, to be very fruitful: it gives full information not only about the DB core sites, but about tail characteristics as well.

Note that the specific structure of a staggered DB core with a central site $n=0$ and two neighboring sites $n=\pm 1$ having amplitudes ϕ_n of opposite signs stipulates several other crossover lengths connected to changes of the sign of the right-hand side in Eq. (14) which manifest as singularities in the logarithmic plots in Fig. 6. The most pronounced crossover at $n=L_2$ is associated with the change from a

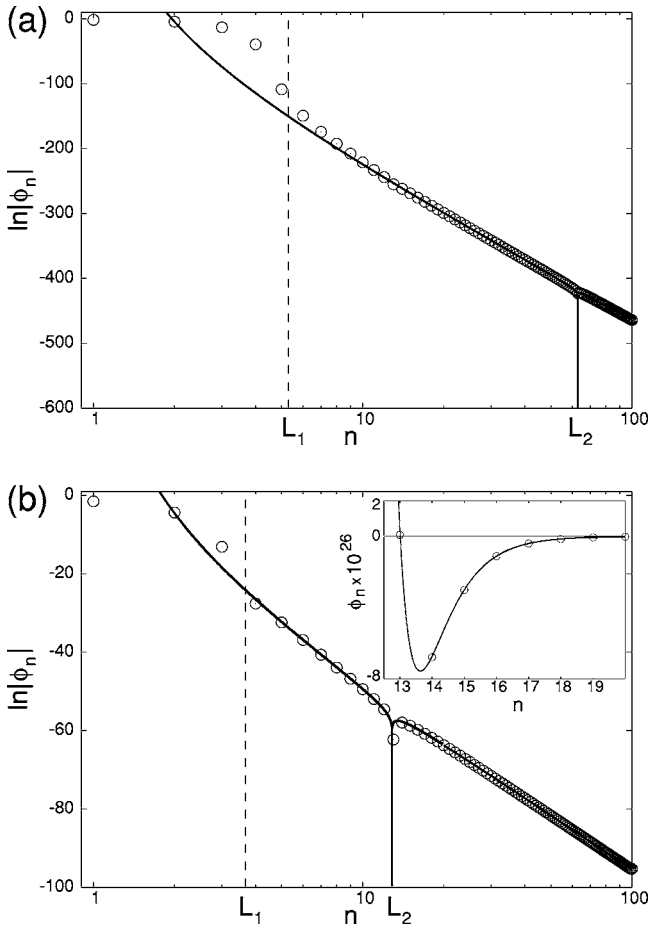

FIG. 6. Single-site H-type DB solutions of Eq. (6) with $C=1$ for various exponents of the long-range interaction: (a) $s=100$; (b) $s=20$. Circles: numerical results. Solid lines: tail asymptotes (14). Dashed lines: location of L_1. The inset in (b) indicates the change of amplitudes sign around the crossover point L_2.

single power law n^{-s} to a more complex one (14), see Fig. 6. Indeed, in the case $n\gg 1$, $(s/n)\ll 1$ the expression (14) can be re-written as

$$\phi_n\approx-\frac{K\phi_0^3}{Cn^s}\left\{1+2\kappa^3+\kappa^3\frac{s^2}{n^2}+o\left(\frac{s^2}{n^2}\right)\right\}, \tag{15}$$

($C=1$, $\kappa<0$ for a staggered core DB and $C=-1$, $\kappa>0$ for a nonstaggered DB). Thus, in leading order, at large enough distance from the DB center $n>L_2$ the tail amplitudes follow the same power law n^{-s} as the decay of long-range interactions. Since L_2 is defined by the vanishing of the bracket on the right-hand side of Eq. (15) we obtain in leading order

$$L_2\approx s\sqrt{\frac{-\kappa^3}{1+2\kappa^3}}. \tag{16}$$

The corresponding values of L_2 for $s=10$, 20, 50, 100, and $\kappa=-0.382$ with Eq. (16) are 5.6, 11.2, 28, 56. They compare reasonably well with the numerically observed ones $L_2(s=10)\approx 7$, $L_2(s=20)\approx 13$, $L_2(s=50)\approx 31$, and $L_2(s=100)\approx 64$. In between the two characteristic length

scales $L_1 < n < L_2$ the tail amplitudes decay following a more complicated power law (14).

V. CONCLUSIONS

To conclude, we revealed the influence of long-range nonlinear interactions on the spatial profile and properties of compactlike discrete breathers in a model of coupled oscillators with pure nonlinear dispersion. As we demonstrate, it is the intriguing property of the model under consideration, that it supports two classes of discrete breathers—with *staggered* and *nonstaggered* spatial profiles of a DB core—having different dynamical properties. The dynamics of a nonstaggered DB is essentially governed by the *soft* nonlinear on-site potential, while DBs with the staggered core have the opposite, *hard*, type of nonlinear dynamical behavior caused mainly by the presence of nonlinear interactions in the chain. Apart from different dynamical properties, the influence of long-range interactions on spatial profiles of these two types of DBs is also different. With the algebraic spatial decay long-range interactions introduce a different length scale which becomes essential at large enough distances from a DB core. We show that the effect of long- and short-range terms competition results in the appearance of a characteristic crossover length L_1 in both types of DBs, at which the spatial tail decay drastically changes from the superexponential law to the algebraic one. For large powers s of the long-range interactions spatial decay the crossover length L_1 scales logarithmically with s. The tail asymptote (14) demonstrates complex power law spatial decay, which follows essentially the same algebraic decay as the long-range interactions in the system at large enough distances from the DB core. While for nonstaggered DBs the influence of long-range interactions manifests through the only characteristic crossover length L_1, the spatial profile of DBs with the staggered core possess several other crossover lengths associated with sign changes of the asymptote (14). Thus the spatial pattern of oscillations in a DB with the staggered core becomes rather complicated in the presence of long-range interactions: its core sites perform antiphase oscillations, while its tails are splitted in several domains of in-phase oscillations.

Finally, we would like to mention that the discussed case of purely nonlinear coupled oscillators represents a simple model to reveal properties of nonlinear excitations in a system without linear phonons. As we demonstrated in this paper, "switching off" the phonons leads not only to the change in characteristic rate of spatial localization of energy, but to appearance of several other intriguing *dynamical* properties of nonlinear localized excitations. Especially it eliminates the possible source of linear resonances which otherwise would destroy quasiperiodic breathers and possibly also moving breathers. The discussed models thus allows us to obtain a better understanding of the general problem of existence or nonexistence of quasiperiodic and moving discrete breather solutions.

ACKNOWLEDGMENTS

We would like to thank M. Johansson for careful reading of the manuscript and providing us with useful comments. We also thank P. Rosenau, T. Bountis, and P. Maniadis for useful and stimulating discussions.

[1] J. S. Russell, in *14th Meeting of the British Association for the Advance of Science* (Murray, London, 1845), pp. 311–390, 57 plates.
[2] S. Aubry, Physica D **103**, 201 (1997); S. Flach and C. R. Willis, Phys. Rep. **295**, 181 (1998); *Energy Localisation and Transfer*, edited by T. Dauxois, A. Litvak-Hinenzon, R. MacKay, and A. Spanoudaki (World Scientific, Singapore, 2004); D. K. Campbell, S. Flach, and Yu. S. Kivshar, Phys. Today **57** (1), 43 (2004).
[3] H. S. Eisenberg, Y. Silberberg, R. Morandotti, A. R. Boyd, and J. S. Aitchison, Phys. Rev. Lett. **81**, 3383 (1998).
[4] A. Sukhorukov, Y. Kivshar, H. Eisenberg, and Y. Silberberg, IEEE J. Quantum Electron. **39**, 31 (2003).
[5] J. Fleischer, M. Segev, N. Efremidis, and D. Christodoulides, Nature (London) **422**, 147 (2003).
[6] E. Trias, J. J. Mazo, and T. P. Orlando, Phys. Rev. Lett. **84**, 741 (2000).
[7] M. Sato, B. E. Hubbard, A. J. Sievers, B. Ilic, D. A. Czaplewski, and H. G. Craighead, Phys. Rev. Lett. **90**, 044102 (2003).
[8] M. Sato, B. Hubbard, L. English, A. Sievers, B. Ilic, D. Czaplewski, and H. Craighead, Chaos **13**, 702 (2003).
[9] M. Sato, B. Hubbard, A. J. Sievers, B. Ilic, and H. Craighead, Europhys. Lett. **66**, 318 (2004).
[10] U. T. Schwarz, L. Q. English, and A. Sievers, Phys. Rev. Lett. **83**, 223 (1999).
[11] M. Sato and A. Sievers, Nature (London) **432**, 486 (2004).
[12] M. Machida and T. Koyama, Phys. Rev. B **70**, 024523 (2004).
[13] I. Kourakis and P. Shukla, Phys. Plasmas **12**, 014502 (2005).
[14] S. Flach, Phys. Rev. E **58**, R4116 (1998).
[15] P. Rosenau and J. M. Hyman, Phys. Rev. Lett. **70**, 564 (1993).
[16] P. Rosenau, Phys. Rev. Lett. **73**, 1737 (1994).
[17] Y. S. Kivshar, Phys. Rev. E **48**, R43 (1993).
[18] S. Flach, Phys. Rev. E **50**, 3134 (1994).
[19] B. Dey, M. Eleftheriou, S. Flach, and G. P. Tsironis, Phys. Rev. E **65**, 017601 (2001).
[20] P. Rosenau and S. Schochet, Phys. Rev. Lett. **94**, 045503 (2005); Chaos **15**, 015111 (2005).
[21] S. Flach and C. R. Willis, Phys. Lett. A **181**, 232 (1993); S. Flach, C. R. Willis, and E. Olbrich, Phys. Rev. E **49**, 836 (1994).
[22] Yu. B. Gaididei, S. F. Mingaleev, P. L. Christiansen, and K. Ø. Rasmussen, Phys. Rev. E **55**, 6141 (1997); M. Johansson, Yu. B. Gaididei, P. L. Christiansen, and K. Ø. Rasmussen, *ibid.* **57**, 4739 (1998); P. L. Christiansen, Yu. B. Gaididei, F. Mertens, and S. F. Mingaleev, Eur. Phys. J. B **19**, 545 (2001).
[23] S. Flach, and A. Gorbach, Chaos **15**, 015112 (2005).
[24] S. Flach, in *Energy Localization and Transfer*, edited by T.

Dauxois, A. Litvak-Hinenzon, R. MacKay, and A. Spanoudaki (World Scientific, Singapore, 2004), pp. 1–71.

[25] T. Cretegny, Ph.D. thesis, École Normale Supérieure de Lyon, Lyon, France, 1998; M. Öster, M. Johansson, and A. Eriksson, Phys. Rev. E **67**, 056606 (2003); A. V. Gorbach and M. Johansson, *ibid.* **67**, 066608 (2003).

[26] D. Chen, S. Aubry, and G. P. Tsironis, Phys. Rev. Lett. **77**, 4776 (1996).

[27] The constant C can be removed from Eqs. (5) and (6) by rescaling $G \to G/\sqrt{|C|}$ and $\phi_n \to \sqrt{|C|}\phi_n$. Note that this rescaling does not affect the initial variables $u_n = G\phi_n$.

[28] The eigenvalues are slightly different due to the noncompact breather profile.

[29] While using the periodic boundary conditions, we introduce a cutoff for the interaction range exactly at one half of the system size, to avoid double counting of interactions.